Miniature Guided Light Array Sequential Scanning Display for Head Mounted Displays

Final Report

Contract No. DAAB07-98-C-G011

Period of Performance: 11/10/97 - 05/15/98

Sponsor:

U.S. Army CECOM
Fort Monmouth, NJ

Technical Monitor:

Charles Bradford
(703) 704-1317

Contractor:

Physical Optics Corporation
Engineering & Products Division
20600 Gramercy Place, Bldg. 100
Torrance, CA 90501

Principal Investigator:

Tin M. Aye, Ph.D.
(310) 320-3088

May 15, 1998

REPORT DOCUMENTATION PAGE

Form Approved
OMB No. 0704-0188

1. AGENCY USE ONLY *(Leave blank)*	2. REPORT DATE	3. REPORT TYPE AND DATES COVERED
	5/15/98	Final Report, 11/10/97-5/15/98

4. TITLE AND SUBTITLE
Miniature Guided Light Array Sequential Scanning Display for Head Mounted Displays

5. FUNDING NUMBERS
DAAB07-98-C-G011

6. AUTHOR(S)
Tin M. Aye, Ph.D., Kevin Yu

7. PERFORMING ORGANIZATION NAME(S) AND ADDRESS(ES)
Physical Optics Corporation
Engineering & Products Division
20600 Gramercy Place, Building 100
Torrance, California 90501

8. PERFORMING ORGANIZATION REPORT NUMBER
3443

9. SPONSORING / MONITORING AGENCY NAME(S) AND ADDRESS(ES)
U.S. Army CECOM
Fort Monmouth, NJ 07703

10. SPONSORING / MONITORING AGENCY REPORT NUMBER

11. SUPPLEMENTARY NOTES

12a. DISTRIBUTION / AVAILABILITY STATEMENT
Approved for public release
Distribution is unlimited

12b. DISTRIBUTION CODE
A

13. ABSTRACT *(Maximum 200 words)*

In Phase I, Physical Optics Corporation (POC) demonstrated the feasibility of Guided Light Array Sequential Scanning (GLASS) display technology for use in low-cost, low-power compact night-vision head mounted displays (HMDs). GLASS is based on a unique combination of three technologies: low-power light emitting diode (LED) arrays; a polymer waveguide array substrate; and liquid crystal micro-optics. POC's display surpasses current HMD displays in terms of size, power, resolution, and speed. This is achieved by direct modulation of high-speed LED arrays to generate line images, and by parallel projection of light through a flexible polymer waveguide array sequentially scanned by means of a liquid crystal output coupler array. Using the MHz speed of LEDs and time-multiplexing, the display is capable of high grayscale and dimming range. The production-phase device will be lightweight, rugged, and compact, and will require little power or maintenance. With its high frame rate and high resolution, it will also reduce time-based and spatial image artifacts.

14. SUBJECT TERMS
HMD, Micro-Optics, Polymer Waveguide, Liquid Crystal

15. NUMBER OF PAGES
34

16. PRICE CODE

17. SECURITY CLASSIFICATION OF REPORT	18. SECURITY CLASSIFICATION OF THIS PAGE	19. SECURITY CLASSIFICATION OF ABSTRACT	20. LIMITATION OF ABSTRACT
Unclassified	Unclassified	Unclassified	SAR

TABLE OF CONTENTS

1.0 INTRODUCTION

1.1 Background

Head mounted displays (HMDs) can sharply increase the effectiveness of combat soldiers -- and their chances of survival. These devices can simultaneously display video, tactical data, thermal imagery, and still graphics [1]. A combat soldier's HMD should operate under lighting conditions from bright daylight to overcast to starlight to full dark, and a soldier on an extended mission needs an untethered, lightweight HMD with low power consumption. Basically, an HMD consists of a miniature image source and display optics. Images come to the display from head-mounted video cameras, thermal imagers, or remote sources. In the past, miniature cathode ray tubes have been the only image sources used in military HMDs.

Recently, new display technologies have emerged as potential alternatives, including liquid crystal displays (LCDs), electroluminescent displays, and several other miniature displays [2,3]. None of these has yet been integrated into a military HMD that meets stringent military requirements and combines acceptable performance, reliability, size, weight, power consumption, and cost. For example, the major weakness of most LCD-based HMDs is that system response is slow, causing time lags, particularly in head- or eye-tracking HMD systems. These time lags can be disorienting, and frequently cause motion sickness. Poor resolution is another important limitation in LCD-based systems. Thus far, efforts to enhance resolution and decrease time lags have been at the cost of low refresh rates and high power consumption; these "enhanced" systems are also more expensive to produce. Additionally, LCD devices are still inefficient, since only a small percentage of the illumination light reaches the image display. As a result, although the LCD itself requires only milliwatts, overall power consumption is typically several watts.

Recently, several new image source approaches based on the direct modulation of light sources have emerged that could overcome the major problems of LCD-based HMDs. Researchers at the Human Interface Technology Laboratory at the University of Washington proposed an approach that bypasses any form of display screen by using acousto-optically (A/O) scanned laser diodes and a mechanical resonant scanner to write images directly on the retina [4]. Although this method works, it offers only a small field-of-view, and requires a bulky, power-consuming scanner, making the device unsuitable for military combat HMDs. Reflection Technology in Massachusetts uses high-resolution linear LED arrays in a small chip (~1 cm long) and a miniature mechanical scanner to create VGA resolution (640 × 480) color images with a contrast ratio of 5000:1, drawing only 250 mW or less [5]. This approach takes advantage of the intrinsic high modulation speed of LEDs, eliminating the need for a display screen and an illumination light source with the associated optics. However, because they require a mechanical scanner, their potential for military HMD use has never been realized.

1.2 POC's Approach

POC's proposed miniature Guided Light Array Sequential Scanning (GLASS) display (see Figure 1-1) consists of three key components:

1. *A Line Image Source Array (LISA),* consisting of a set of three-color (RGB) LED linear arrays integrated with a micro-optic/diffractive optical element (DOE) input coupler for LED light beam forming and coupling for each column of the display.
2. *A flexible Polymer Waveguide Array Substrate (PWAS),* consisting of a highly parallel step index or graded index channel waveguide array to project parallel line images.
3. *A Liquid Crystal Output Scanner (LCOS) array,* consisting of a linear array of LC microprisms or LC diffractive micro-optics, for efficient output coupling and display of line images.

The unique combination of these three components gives the GLASS display system a clear performance edge over state-of-the-art displays.

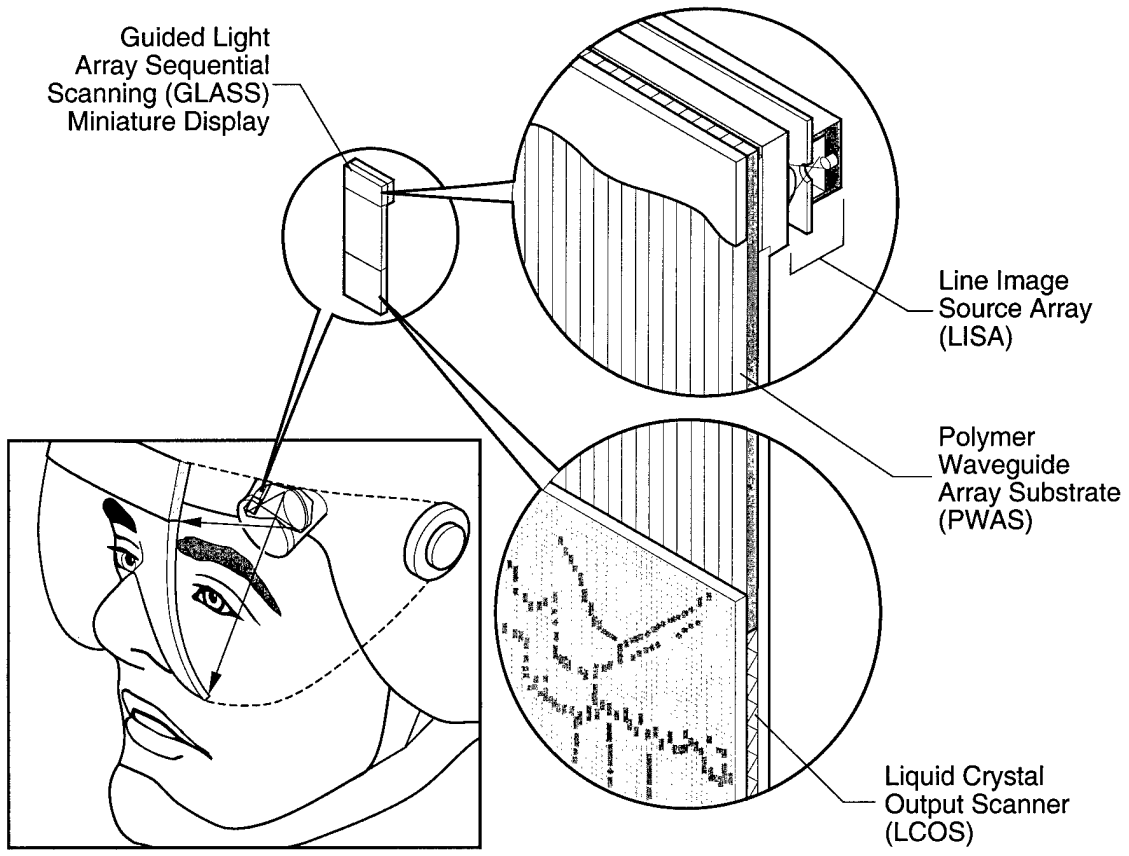

Figure 1-1
POC's proposed Guided Light Array Sequential Scanning (GLASS) miniature display for use in a high-performance, rugged, lightweight, low-power HMD.

POC's new miniature display technology developed in Phase I combines the best characteristics of direct modulation displays and LCDs. This unique combination overcomes the drawbacks of each technology, and is made possible by POC advances in polymer waveguide diffractive optics, liquid crystal micro-optics, lithography, and thin film embossing. In Phase I, POC demonstrated the feasibility of a novel miniature GLASS display for use in military HMDs. The production-phase GLASS displays will be compact and lightweight, require very little power, and have a high frame rate.

This report describes the Phase I work and its results. Section 2 summarizes the results, followed by technical discussion of these results in Section 3. Section 4 presents the conclusions and recommendations for future work, applications and commercialization plans for the GLASS display technology are described in Section 5.

2.0 RESULTS OF PHASE I WORK

2.1 Phase I Objectives

The purpose of the Phase I project was to demonstrate the feasibility of a Guided Light Array Sequential Scanning (GLASS) miniature display to be used in military head mounted display systems. The Phase I technical objectives were:

1. Analyze design and performance of the proposed GLASS miniature display for HMD applications
2. Investigate methods of fabricating Line Image Source Array (LISA), Polymer Waveguide Array Substrate (PWAS), and Liquid Crystal Output Scanner (LCOS) components for the proposed miniature display.
3. Demonstrate the feasibility of the proposed concept by fabricating a proof-of-concept device and evaluating its functionality using an experimental functional setup.

By the end of Phase I, POC had accomplished all objectives and successfully demonstrated feasibility through analytical modeling and computer raytracing as well as experimental proof-of-concept component fabrication and functional demonstration.

2.2 Summary of Phase I Results

In Phase I, POC conducted initial design studies and an experimental demonstration of the key components of the GLASS display. The results show efficient input light coupling from the LISA, propagation through the PWAS, and output coupling from the LCOS, offering a strong proof of

feasibility of the GLASS display concept. Results of this investigation also show a well-defined growth path to high resolution, low power, high performance miniature displays for Army night vision HMDs. They also show that currently available materials and components can be combined with POC's unique micro-optics polymer fabrication technology to manufacture the device at low cost.

In summary, POC can point to six major accomplishments in this Phase I project:

- Completed preliminary design and analysis of GLASS display by computer 3-D modeling and ray-tracing to study light propagation.
- Demonstrated fabrication of LISA components based on a commercial LED array and efficient input coupling.
- Demonstrated PWAS fabrication using commercial photopolymer materials, including DuPont no-dye photopolymer for channel waveguide fabrication.
- Developed LCOS design and fabrication process to demonstrate LC-refractive output scanner (LC-ROS) and LC-diffractive output scanner (LC-DOS) fabrication and to demonstrate LC-ROS (bending) and LC-DOS (diffraction) output.
- Demonstrated integration of a GLASS proof-of-concept experimental unit.
- Explored the commercial potential of GLASS displays.

2.3 GLASS Display Design and Analysis

Figure 2-1 illustrates the conceptual design of the GLASS display, consisting of three key functional components: (1) A *line image source array* (LISA), consisting of linear arrays of LEDs (see Figure 3-8 in Section 3.2) integrated with a micro-optic/diffractive optical element (DOE) input coupler for generating a column (a line) of the display; (2) A flexible *polymer waveguide array substrate* (PWAS), consisting of a channel waveguide array to project a sequence of line images; and (3) a *liquid crystal output scanner* (LCOS) array, consisting of a linear array of LC microprisms or LC diffractive micro-optics for efficient output coupling and precise display of line images.

To accomplish the **first objective**, POC prepared a preliminary design and conducted an experimental performance analysis of these key components, and then developed an initial working model for Phase II prototype development. Specifically, we used OptiCAD computer ray tracing to model ray propagation, and used 3-D waveguide computer modeling software to simulate wave propagation based on the available material and component parameters, and to determine display performance.

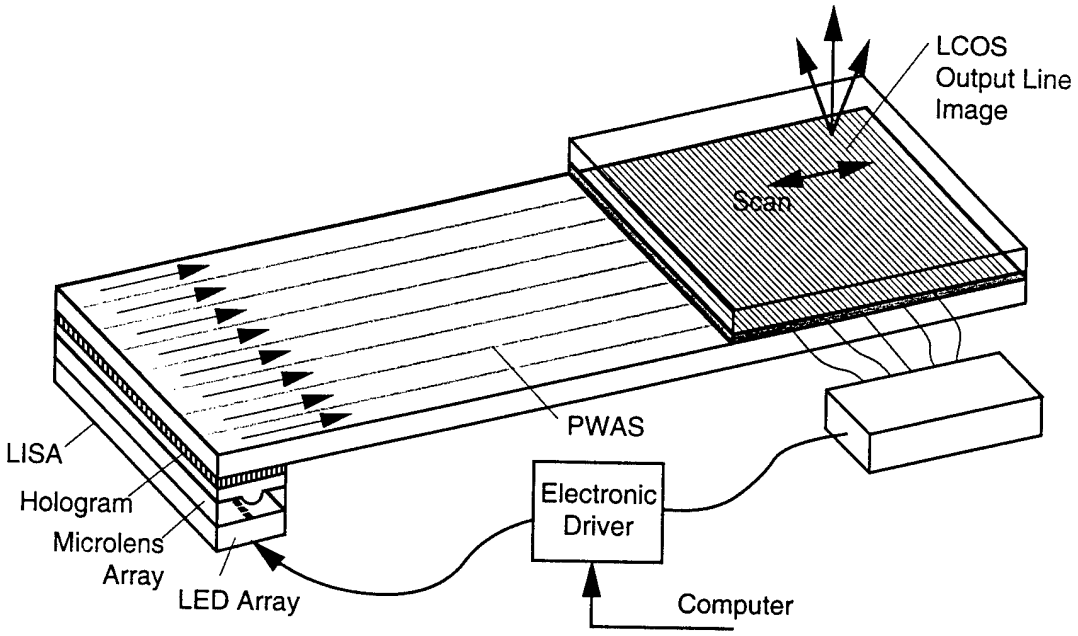

Figure 2-1
Guided Light Array Sequential Scanning design.

For Phase I, a 20 μm × 20 μm 256 pixel linear LED array was procured from Reflection Technology, Inc., for use in the LISA (see Figure 3-8 below). The LED source size and spacing determines the channel waveguide size, spacing, and efficiency of light propagation through the PWAS. Within the constraints of available polymer waveguide parameters (i.e., the refractive index n of the waveguide and buffer), the light propagation efficiency was found to depend on the input coupler model. The size and angular divergence of LED sources are the keys to efficient propagation. The source size should be small compared to the waveguide input aperture.

Input coupling from the LISA to the PWAS was subjected to thorough 3-D wave propagation analysis. The analysis, which assumed no loss and realistic waveguide parameters, determined the propagation mode allowed (acceptance angle or numerical aperture) and light intensity at the output of the PWAS (see Figure 2-2). The results show that efficient propagation can be achieved with negligible cross talk and loss through the waveguide cladding, for all three colors. In a real waveguide, however, a few percent loss is to be expected from absorption and scattering at interfaces.

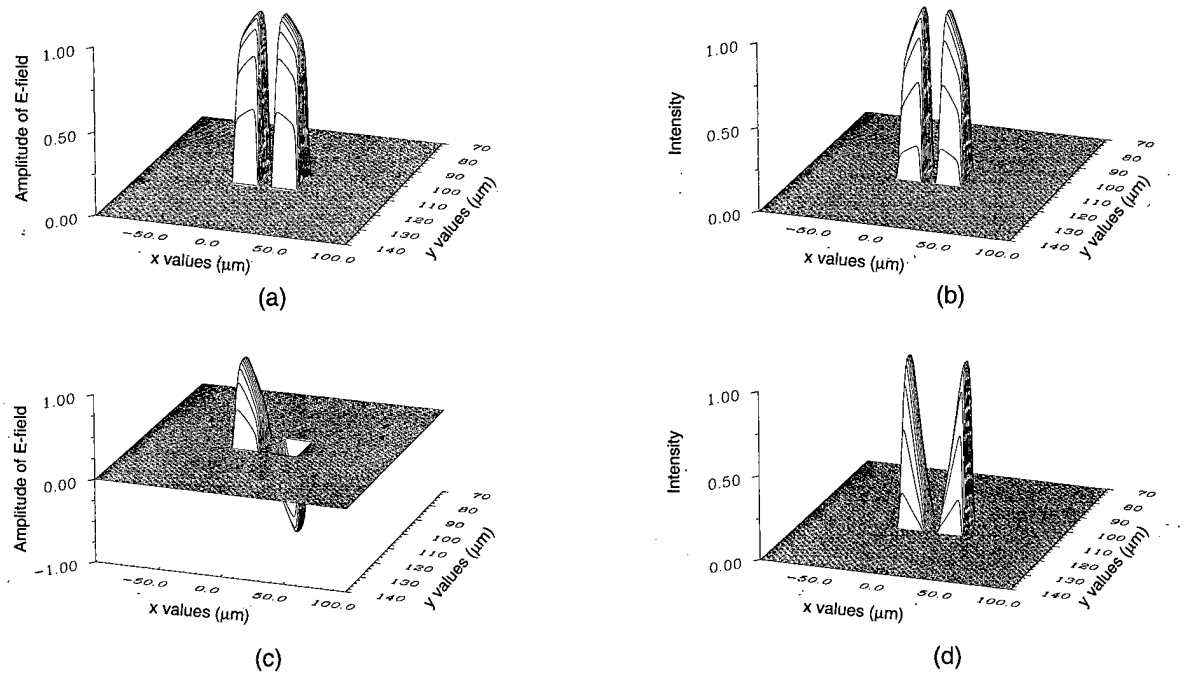

Figure 2-2
A result of 3-D computer modeling of light propagation through a channel waveguide array; normalized amplitude and intensity for TE waves; number of waveguides = 2; wavelength = 0.515 μm; n_{wg} = 1.53; wwg = 20 μm; t_{wg} = 10 μm; n_b = 1.41; w_b = 11.75 μm; $n_{coating}$ = 1.41; $t_{coating}$ = 100 μm. (a) and (b): mode order = 0; modal index = 1.529765. (c) and (d): mode order = 1; modal index = 1.529759.

In a parallel effort, we developed a ray tracing model based on the same waveguide parameters for efficient input coupling, propagation, and output coupling. Several versions of the model were analyzed. At the end of a 2 in. long PWAS, light output was measured at the cross section (detector 1) and at the top surface of a channel waveguide (see Figure 2-3(a)). The results are shown in Table 2-1. Sample ray-tracing results for model 5 are shown in Figure 2-3(b). Using butt-coupling model, several output coupler configurations were studied, including LC micro-prism (LC-ROS), DOE diffuser with LC cladding, and LC micro-prism with a DOE on one prism face. The results show that the latter option is the most efficient LCOS configuration (see Figure 2-3(c)). This analysis led to a Phase I demonstration LISA directly butt-coupled to the edge of the PWAS.

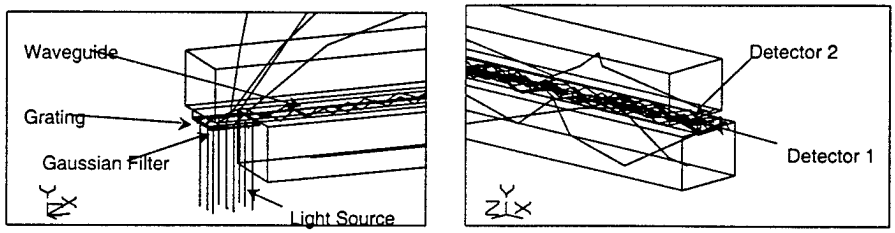

(a)

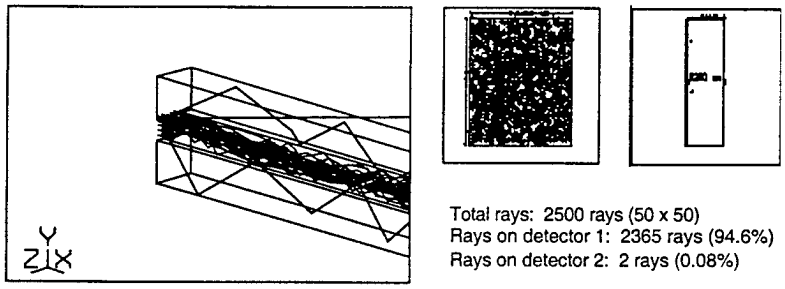

(b)

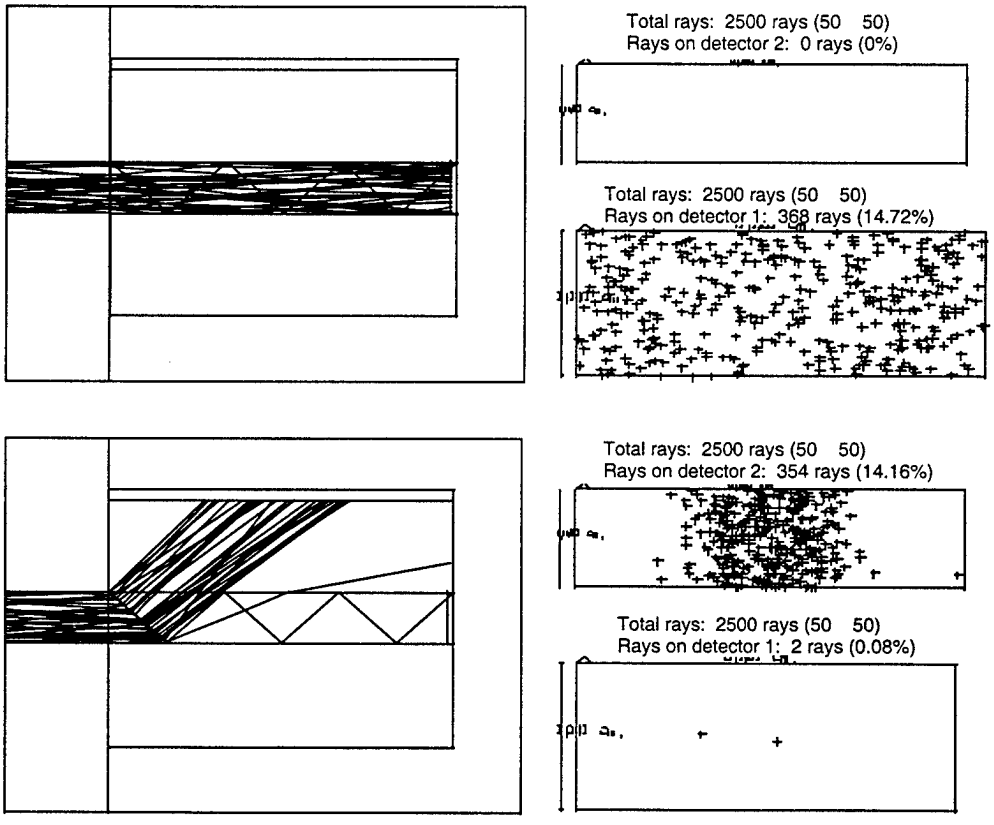

(c)

Figure 2-3
(a) Ray tracing of LISA-to-PWAS coupling. The LED light source is: size = 19 μm x 22 μm, λ = 655 nm, divergence angle = ±60°. (b) Sample ray-tracing of Model 5, with LED coupled directly to waveguide. (c) Ray tracing of waveguiding and LCOS output coupling at display end of PWAS.

Table 2-1. Result of Input Coupling and Light Propagation Analysis (values are numbers of rays)

Input Coupling Model	Detector 1	Detector 2
1. Grating and microprism (f = 1500 ℓ/mm)	225 (9.00%)	104 (4.16%)
2. Grating and microprism (f = 1000 ℓ/mm)	152 (6.08%)	110 (4.40%)
3. Grating only (f = 1500 ℓ/mm)	263 (10.52%)	169 (6.76%
4. Grating only (f = 1000 ℓ/mm)	222 (8.88%)	111 (4.44%)
5. LED butt-coupled to waveguide	**2365 (94.6%)**	**2 (0.08%)**

2.4 GLASS Display Component Fabrication

To meet the **second objective**, POC investigated methods of fabricating the LISA, PWAS, and LCOS components. For the LISA, a Reflection Technology, Inc. P5 256-element LED array was directly butt-coupled into a 20 μm thick polymer waveguide. We investigated two approaches for PWAS fabrication using DuPont no-dye polymer waveguide: (1) holographic recording using two-beam interference, and (2) lithographic contact printing using a mask.

First, the DuPont no-dye photopolymer was thoroughly characterized in terms of its laser-induced refractive index modulation (Δn) and its light transmission properties at multiple wavelengths in the visible region. DuPont no-dye material can have a maximum Δn of 0.03 to 0.04 (see Figure 2-4), which is important for good propagation in channel waveguides. Also, its absorption is very low across the whole visible region (see Figure 2-5), as is necessary for efficient light delivery. The film tested was 20 μm thick, and the spectrophotometer beam was ~2 mm in diameter. Based on this, the maximum loss at 470 nm (i.e., blue light) in a 6 in. long 20 μm × 20 μm waveguide would be only 5%. POC has demonstrated fabrication of channel waveguide structures by holographic recording (see Figure 2-6). The laboratory demonstration of this waveguide is shown in Figure 2-7.

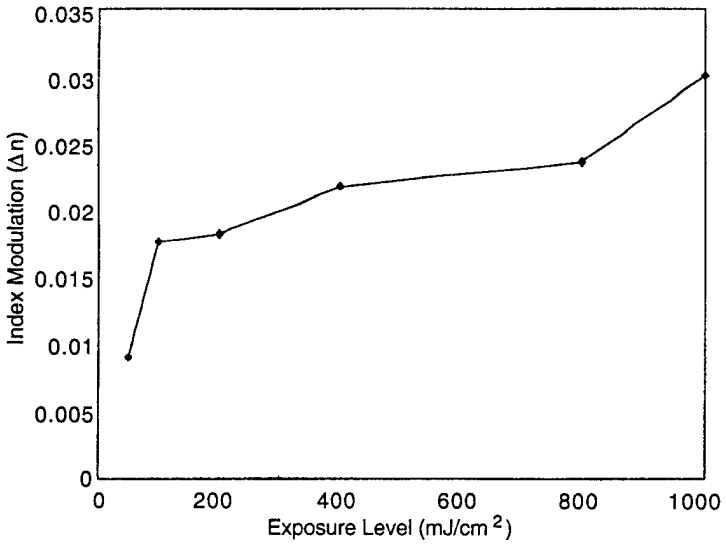

Figure 2-4
Refractive index modulation characteristic of the DuPont no-dye photopolymer film.

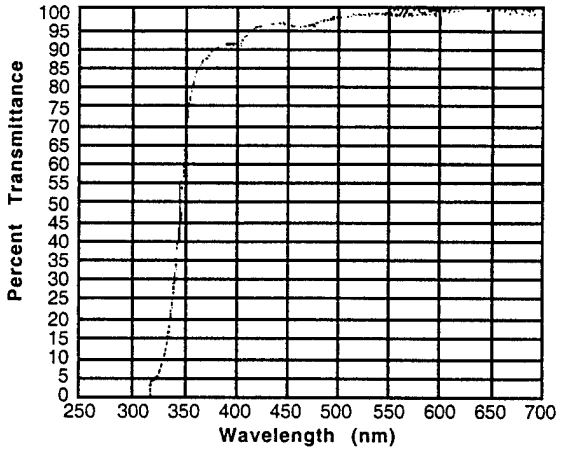

Figure 2-5
Spectral transmittance of no-dye DuPont film. Film thickness = 20 μm; beam size = 2 mm diameter; absorption volume = $\pi(1)^2$ x 0.02 mm^3 = 0.06 mm^3. For 20 μm x 20 μm, absorption length = (0.0628/(0.02x0.02))=157 mm; i.e., maximum 5% loss (near 470 nm) in 15.7 cm (~6 in.) waveguide.

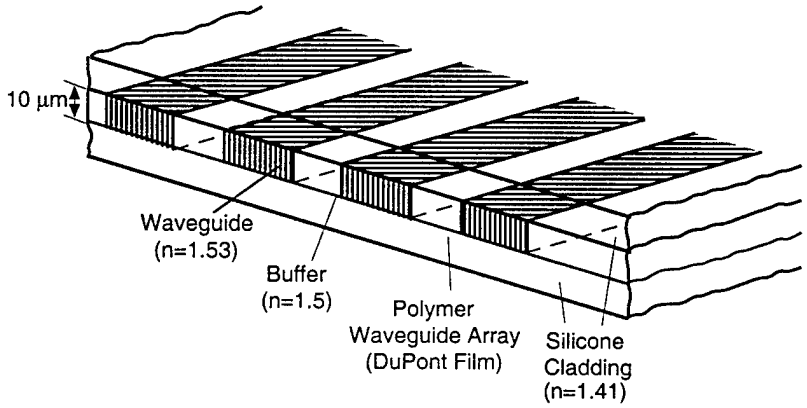

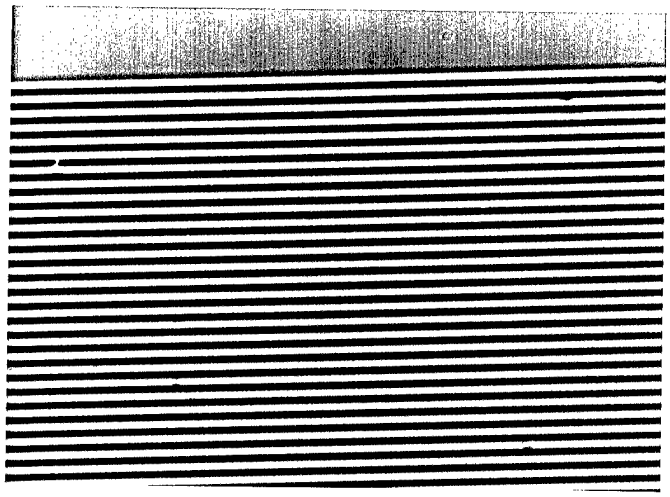

Figure 2-6
Holographically fabricated channel waveguide array with 20 μm channel width, and n_{WG} = 1.53 - 1.54, n_c (cladding) = 1.5.

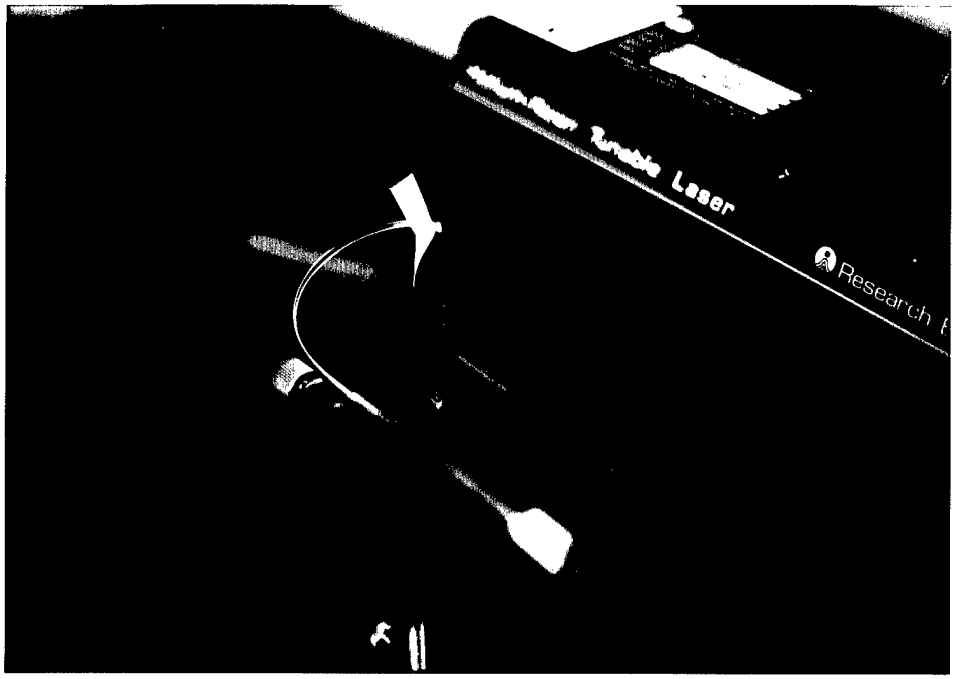

Figure 2-7
Light propagation through PWAS channel waveguides.

Another important area of the work to meet the second objective was to investigate, develop, and fabricate an LCOS module. We studied both refractive (LC-ROS, Figure 2-8(a)) and diffractive (LC-DOS, Figure 2-8(b)) types, and developed and tested various ways of integrating polymer waveguide with an LC cell in preparation for the concept demonstration. We purchased and investigated four LC materials and cell configurations (nematic and ferroelectric LC, varying in alignment direction and thickness). As the result, a unique method was successfully developed for fabricating very thin microprism arrays and diffractive/diffuser microstructures inside LC cells by optimized epoxy-based replication, based on our proprietary techniques.

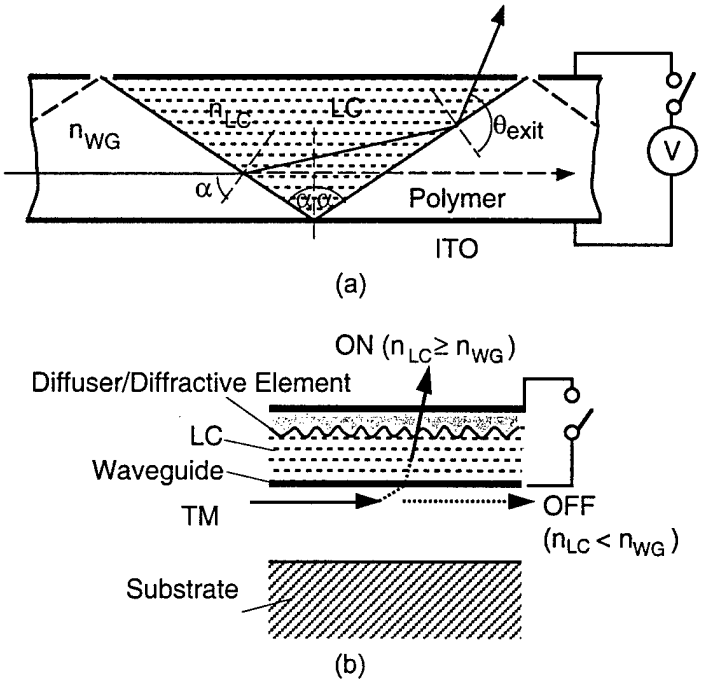

Figure 2-8
LCOS configurations: (a) Refractive coupling, with light output switching by refraction and total internal reflection, and (b) Diffractive coupling, in which nematic liquid crystal is clad on PWAS waveguide. Light output switching occurs when $n_{LC} \geq n_{WG}$.

Merck E7 nematic LC material was used to investigate LCOS fabrication. Refractive coupling by light bending was first studied by replicating polymer micro-prisms in LC cells. Through a major effort, we produced very thin polymer micro-prism arrays using an available 50 μm $\times$ 50 μm acrylic micro-prism array master from Fresnel Optics, Inc. Samples were fabricated and their beam bending characteristics tested. The results showed bending of light as predicted by theoretical analysis. Specifically, a small HeNe laser beam was launched into the substrate and guided in total internal reflection (TIR) waveguide mode. The beam remained inside the substrate unit until a small voltage was applied to bend the light out of the unit.

Similar experiments were carried out using a thin surface relief diffuser (POC light shaping diffuser) replicated inside an LC cell. The light again propagated in TIR mode until a small applied voltage diffused the light out of the substrate. POC considers the LCOS demonstration successful.

Part of this objective was to demonstrate that the LCOS can meet the 100 μs speed requirement for the GLASS display. The fastest reported TNLC material switching time is ~1 ms to 500 μs, while ferroelectric LC material has demonstrated times of ~30 μs to 100 μs (see Figure 2-9), though FLCs are more sensitive to temperature variation than NLCs. However, according to several manufacturers of FLC materials (e.g., Hoechst in Germany and Rolic in Switzerland), a variety of FLCs can operate within a relatively wide temperature range, from -40°C to 70°C, without it substantially affecting their speed or birefringence. Thorough testing of FLC-based LCOS units at these temperatures will be conducted in future development.

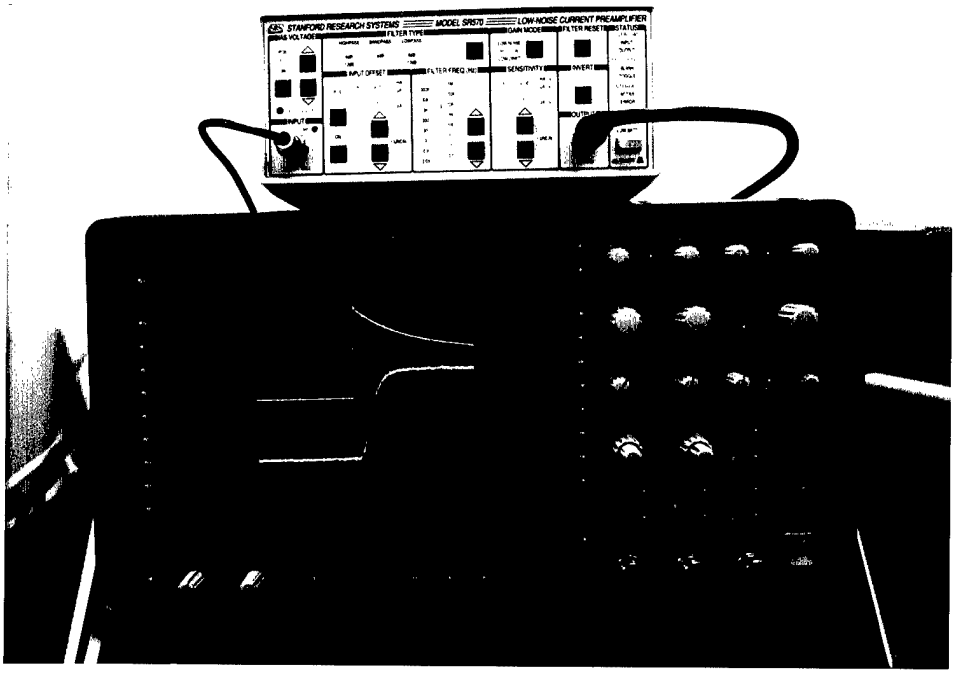

Figure 2-9
FLC switching speed of <50 μs demonstrated at POC.

2.5 GLASS Display Concept Demonstration

POC met the **third objective** by conducting several experiments to show the individual component functions, and through laboratory simulation of an integrated LISA, PWAS, and LCOS (see Figure 2-10) to demonstrate the proposed GLASS concept.

As a GLASS concept demonstration, an LED array, a 50 μm thick polymer waveguide coated with ITO, and a surface relief diffuser forming a pattern in an NLC cell were set up on precision

mounting stages to form a display unit. The unit demonstrated LED light coupling and propagation along the polymer waveguide, and output coupling of light in response to a low voltage applied to the cell (see Figure 2-10). This demonstration unit clearly proved the basic concept, showing a high degree of feasibility for Phase II development.

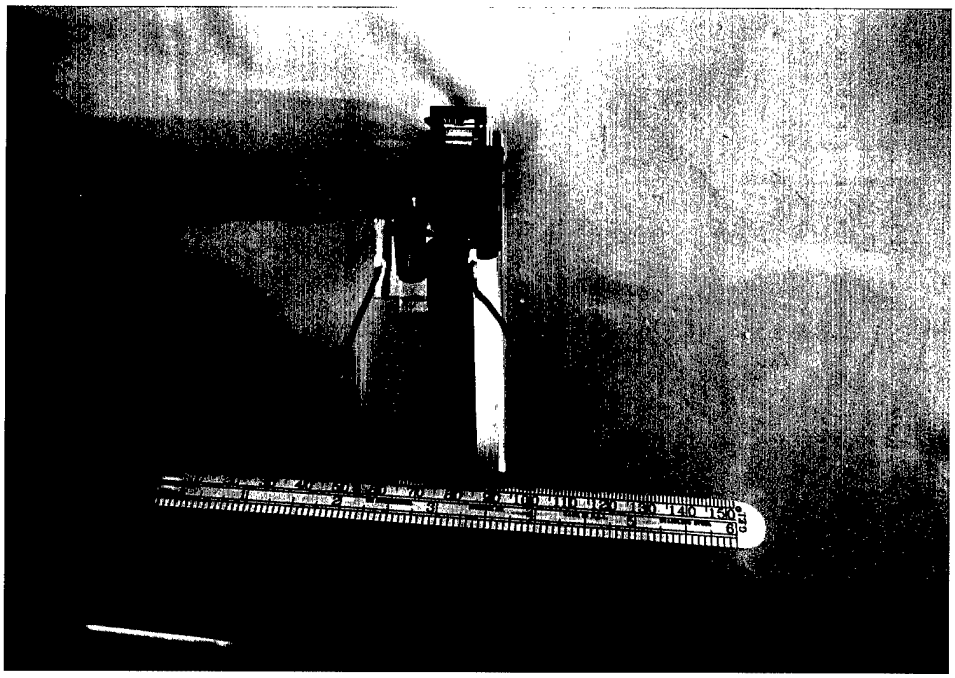

Figure 2-10
GLASS display concept demonstration laboratory setup.

In the course of the Phase I studies, POC also conducted a preliminary survey of the commercial potential of GLASS displays. This involved establishing initial contacts with companies interested in using GLASS displays, as well as those interested in participating in the development of this technology for specific commercial markets.

Summary. The Phase I investigations have demonstrated that a practical commercially viable miniature display can be developed based on POC's novel GLASS display concept. A high resolution version of this unit can be designed, fabricated, and manufactured for Army land warrior night vision HMDs, and for high end commercial uses such as medical HMDs, and a lower-priced version for major commercial applications. POC believes that development of a full scale GLASS display will lead to the most advanced and lowest cost HMD yet developed.

3.0 GLASS DISPLAY TECHNOLOGY

The technology responsible for the Phase I results summarized in the previous section is discussed here in some detail.

3.1 Design and Analyze GLASS Display

The GLASS design was developed based on currently available components and materials. Analytical modeling, computer ray tracing, and simulation were used in a thorough analysis. Component parameters for the LISA, PWAS, and LCOS were then determined. The design was made compatible with current HMD optics and sensors, to address the Army's immediate HMD needs and requirements.

In Phase I, only a red LED array was used. Blue and green LED arrays were studied for future implementation. The parameters of other components were projected from those of the red LED array.

3.1.1 Key Design Issues

Resolution

The resolution of the display can be very high, since several LISA arrays can be multiplexed using the PWAS into a combined high resolution array. Each channel of the polymer waveguide can be as small as the size of an LED element. With a 20 μm channel waveguide, a 1024 × 1024 display will be only about 2 cm wide.

Column resolution is determined by the height-to-width ratio of the LC microprism, which is ~1:1. Since LC cell thickness must be < 20 μm to keep the driving voltage low, the pixel sizes will also be ~< 20 μm. Therefore, a 1024 × 1024 display will be ~ 2 cm × 2 cm.

Light Power Budget

The total light power budget can be >50%. This is due to the efficient light coupling of the DOE and micro-optics. Also, little light is lost through the polymer waveguide substrates, and nearly 100% of the light is coupled by the LCOS array at the display end. In multimode systems, highly efficient coupling is routinely achievable. Even though some loss of light is inevitable at interfaces -- Fresnel losses and scattering from edges of micro-optic arrays -- the overall power budget can be well above 50%.

Response Time/Refresh Rate

Since an LED array can be modulated at several hundred MHz, the response time, or refresh rate, of the proposed GLASS miniature display is determined by the scanning speed of the LCOS, i.e., the turn-on speed of the LC material forming the LC microprism. For a typical twisted nematic LC display, response time is ~30 ms. New nematic LC materials show faster switching speeds, ~1 ms, while the state-of-the-art analog ferroelectric LC material (DHFLC) has demonstrated μs switching speed. With these materials, the frame refresh rate can range from 1 kHz to 30 kHz.

Since both LED arrays and the LCOS are electrically addressed in parallel, the usual speed bottleneck caused by matrix addressing in conventional LCDs does not exist.

3.1.2 3-D Waveguide Model

Physical Optics Corporation uses the Alternating Direction Implicit (ADI) method for three-dimensional waveguide analysis. In our coordinate system, the direction of propagation is along the positive z-axis. The ADI method calculates both the propagation constants and modal fields for index profiles in two transverse dimensions (i.e., x-axis and y-axis). The ADI method for solving the semivectoral Helmholtz equations determines all propagation constants and mode eigenfunctions. The basic idea of the ADI method is to separate the x and y derivatives in two parts of one iteration step. The first kind of boundary conditions are the homogeneous boundary conditions (Dirichlet), where the dependent variable vanishes at all the boundaries. The second kind are the Neumann boundary conditions, where all the normal derivatives of the dependent variable vanish at the boundaries [6,7]. By default, Neumann boundary conditions are applied. The results show that efficient propagation can be achieved with negligible cross talk and loss through the waveguide cladding, for all three colors. In a real waveguide, however, a few percent loss is to be expected from absorption and scattering at interfaces. The initial result of this analysis is shown above Figure 2-2. The analysis shows the wave propagation characteristic of the PWAS, and is useful in detail modeling of the input and output couplers, which will be conducted in a future phase of development.

3.1.3 Ray Tracing Models

In a parallel effort, we developed a ray tracing model based on the same waveguide parameters used in the analytical simulation and 3-D waveguide analysis. Different versions of the model were analyzed and compared. We used Z-MAX to study the models in terms of light coupling from an LED source, propagation along the length of a channel waveguide, and light output by the LCOS. An LED with a source area of 20 μm × 20 μm and a divergence angle of ~45° - 60° in air was used, together with waveguide parameters as defined by our design. Light input coupling was first analyzed using a microprism array and holographic gratings with different grating periods. Although this method would be ideal for a pointlike source, the size and divergence angle of the LED cause inefficient light transmission -- a maximum efficiency of ~10%. In the second approach, the LED source was directly butt-coupled into a channel waveguide, with light efficiency of up to ~90% (see Figures 3-1 through 3-6). The second approach was used in the demo unit.

In these analyses, light output was determined at the cross section (detector 1) and at the top surface of a channel waveguide (see Figure 3-1).

PWAS Parameters

Refractive Indices:
Waveguide n_w = 1.53 (DuPont)
Cladding n_c = 1.41 (silicone)
Thickness:
Waveguide h_w = 10-25 μm
Cladding h_c = 50 μm

Lengths
Waveguide Lw = 50 mm
LED Source: 19 μm× 22 μm
LED Wavelength: 655 nm
LED Divergence: ±30° in medium

- This report summarizes the ray tracing for Miniature Guided Light Array Sequential Scanning Display for Head Mounted Displays
- The Model of ray tracing are :
  1) f=1500 grating & microprism
  2) f=1000 grating & microprism
  3) f=1500 grating only
  4) f=1000 grating only
  5) LED direct attach to WG
- The summarized results are :

Model	Total rays	detector 1	detector2
1)	6000	225(9.00 %)	104(4.16 %)
2)	6000	152(6.08 %)	110(4.40 %)
3)	6000	263(10.52%)	169(6.76 %)
4)	6000	222(8.88 %)	111(4.44 %)
5)	6000	2365(94.6%)	2(0.08 %)

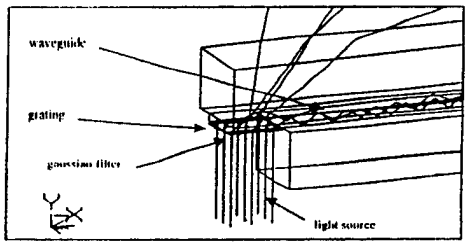

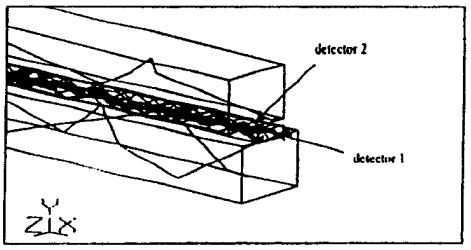

Figure 3-1
Summary of PWAS ray tracing results.

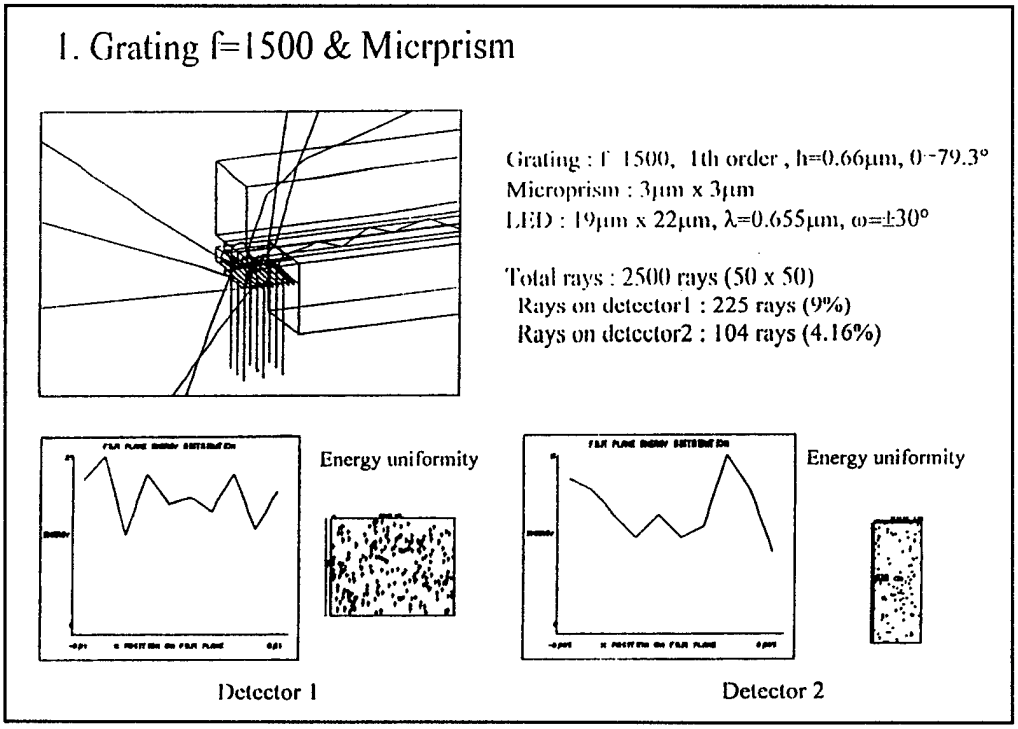

Figure 3-2
Case 1: Input coupling using grating and microprism.

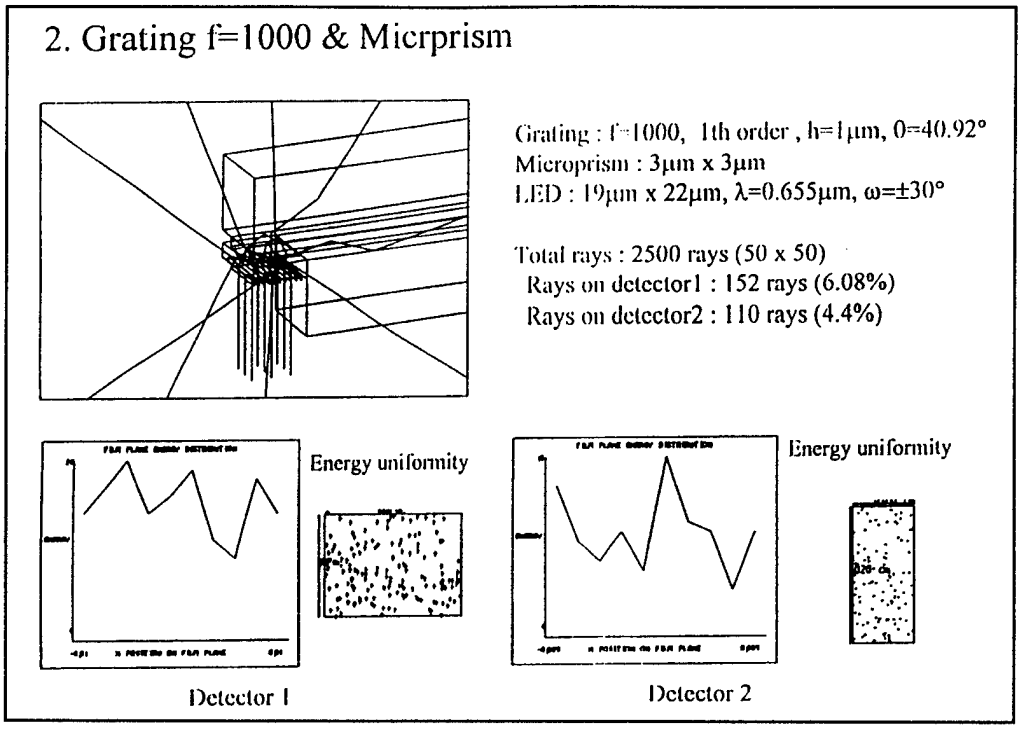

Figure 3-3
Case 2: Input coupling using grating and microprism.

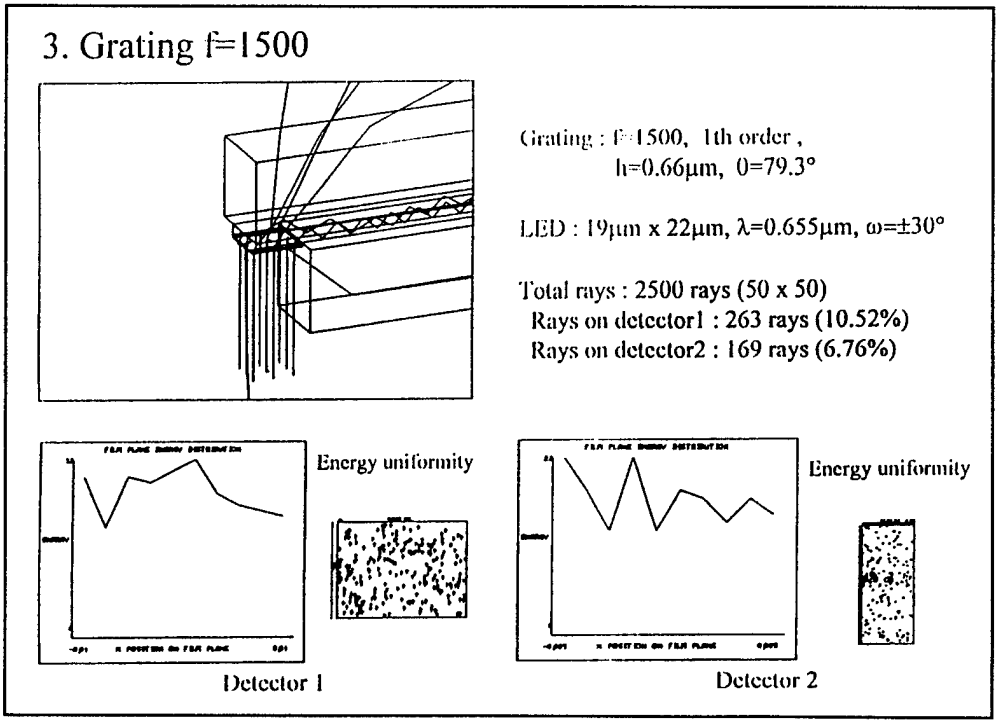

Figure 3-4
Case 3: Input coupling using only grating.

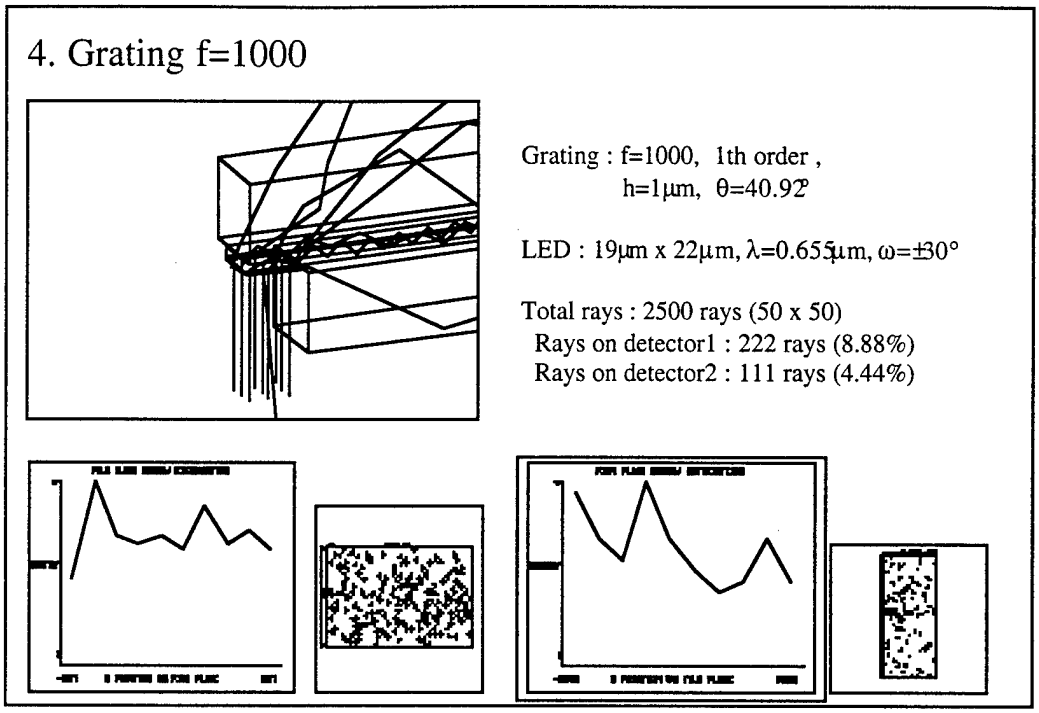

Figure 3-5
Case 4: Input coupling using only grating.

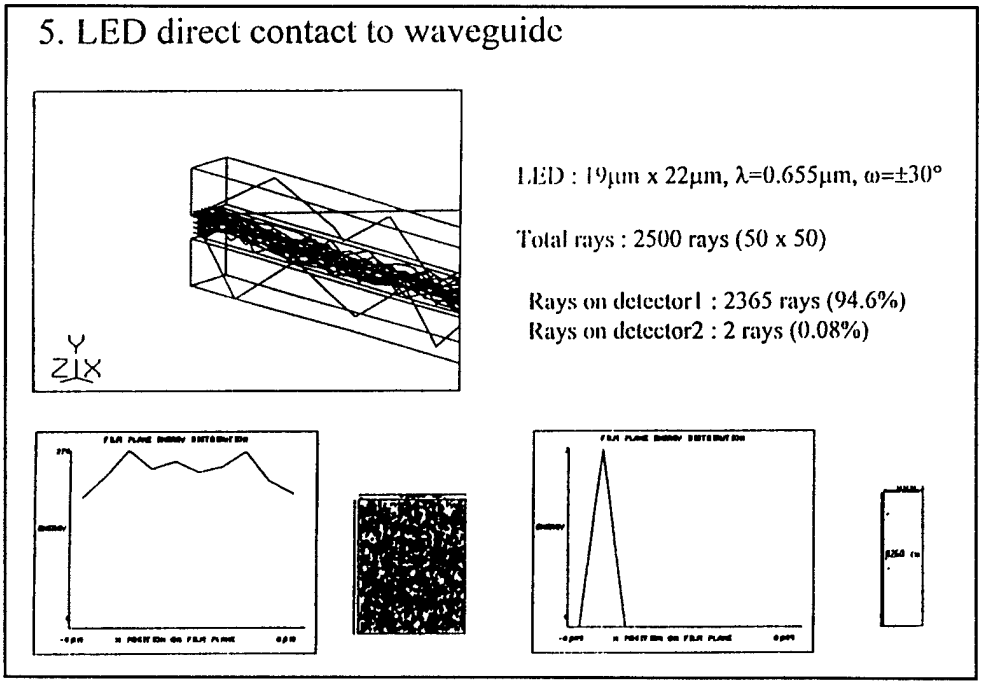

Figure 3-6
Case 5: Direct butt-coupling from the edge.

Using a butt-coupling model, several output coupler configurations were studied, including LC micro-prism (LC-ROS), DOE diffuser with LC cladding, and LC micro-prism with a DOE on one prism face. The results show that the latter option is the most efficient LCOS configuration (see Figure 3-7).

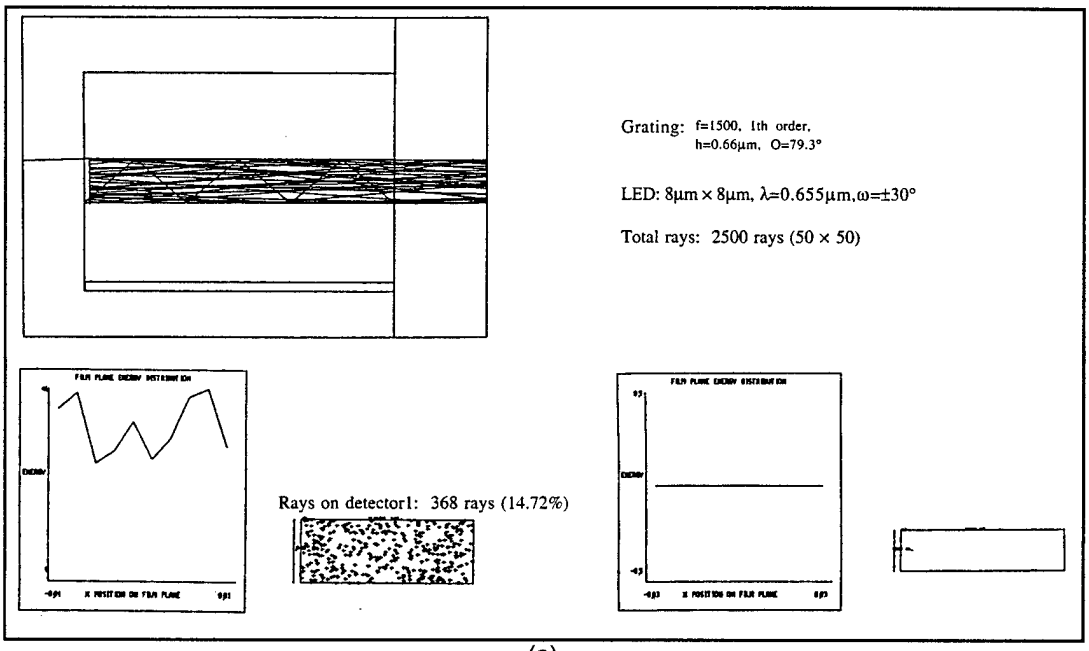

(a)

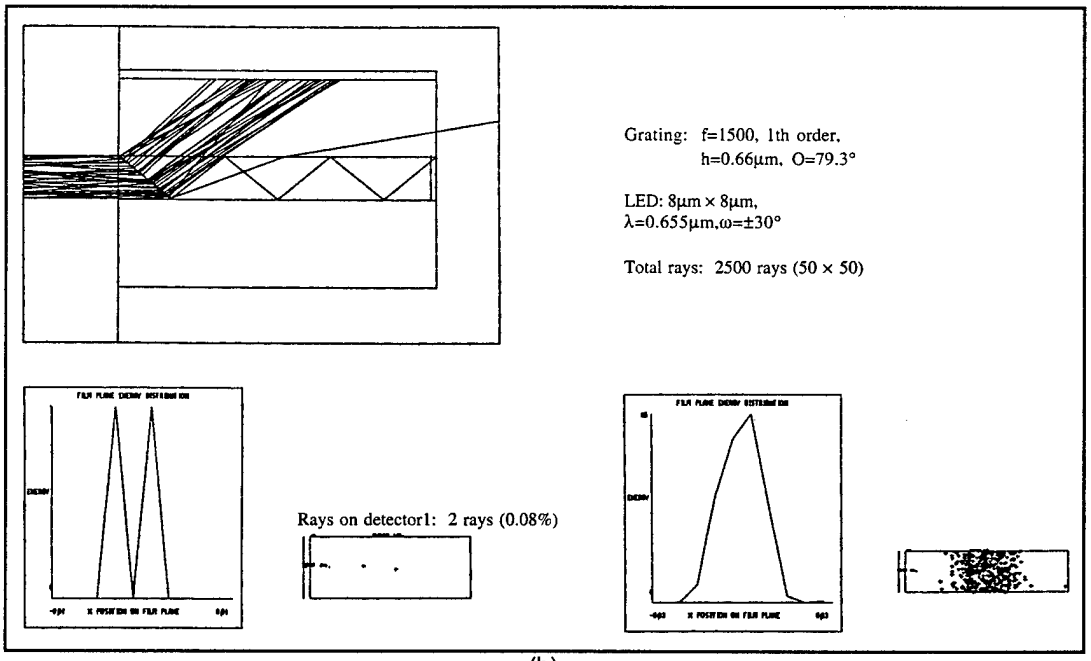

(b)

Figure 3-7
Ray tracing of waveguiding and LCOS output coupling by varying LC refractive index with a surface relief grating on the input face of LCOS elements. (a) LCOS element in switch-off mode ($n_{LC}=n_{WG}$); and (b) LCOS element in switch-on mode ($n_{LC}>n_{WG}$).

3.2 Fabrication of LISA

In the LISA, POC used a commercial linear LED array from Reflection Technology, Inc. The initial effort focused on a monochrome red device (P5) with a resolution of 256 pixels. Reflection Technology has recently released a VGA resolution, full RGB miniature display (640 × 480) using their mechanical scanner. POC has analyzed this new device for future high-resolution GLASS display development. Table 3-1 shows the typical parameters of the currently available P5 red linear LED arrays (see Figure 3-8).

Table 3-1. LED Array Specifications

Active Array Length	8.09625 mm ± 0.020 mm
Number of Emitters	256 dots
Emitter size	19 × 22 μm (with a stripe electrode)
Emitter Pitch	31.75 μm
Emitter Pitch Error (x)	±5 μm (inside a chip)
Emitter Height Linearity	50 μm max (overall)
Emitter Height from Mount Surface	0.35 ± 0.1 mm (overall)
Module Dimensions	16 (L) × 27 (W) × 4.7 (H) mm
Light Peak Wavelength	655 ± 10 nm (T_A = 20°C, I_{LED} = 1.5 mA)
Luminous Intensity	0.7 - 1.3 μW

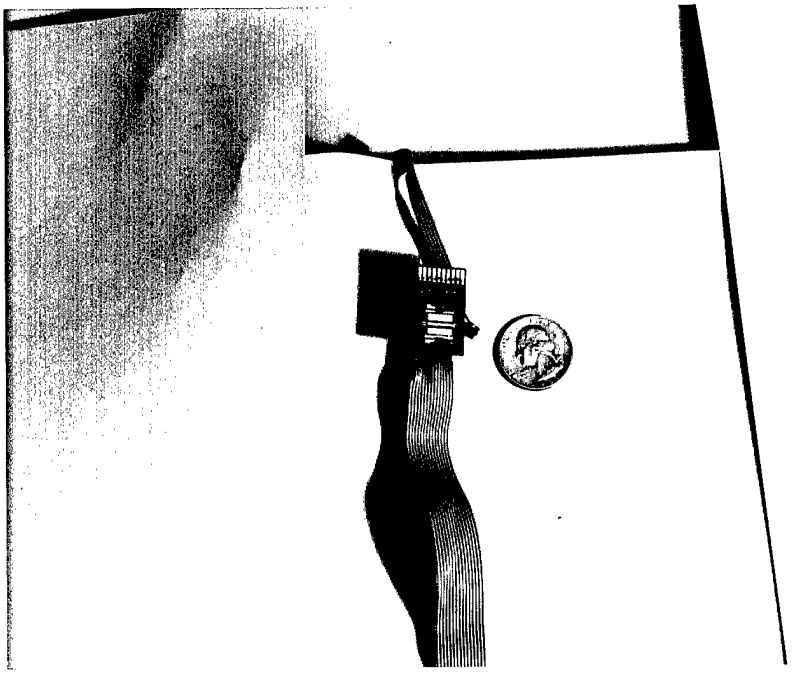

Figure 3-8
Reflection Technologies P5 LED array.

3.3 Fabrication of PWAS

Two PWAS fabrication techniques were investigated: holographic and lithographic. The holographic method controls the interference of two laser beams to produce fringe patterns ~10-20 μm wide. A thin film (~10 μm) DuPont photopolymer (DPP) material was used to record the fringe patterns produced by two interfering laser beams (at 413 nm). The patterns are then converted into a material index variation Δn after UV exposure and baking (see Figure 3-9) in the form of parallel arrays, which form the required channel waveguide array. Graded index type (rounded square) waveguide arrays were fabricated using POC's proprietary recording technique, based on the non-linear response of the recording materials. In order to determine the achievable index modulation Δn of the PWAS, the DPP material was characterized by using a single beam to record Lippmann reflection holograms.

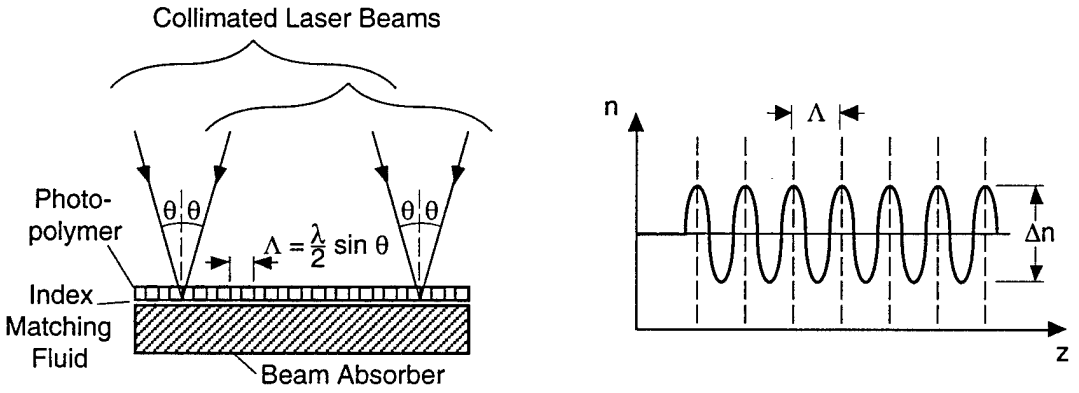

Figure 3-9
PWAS fabrication by volume holographic nonlinear recording.

Index modulation Δn of a Lippmann reflection hologram can be predicted using Kogelnik's formula [8]:

$$\eta = \tanh^2\left(\frac{\pi \cdot \Delta n \cdot d}{\lambda_o}\right)$$

$$\Delta n = \frac{\lambda_o \tanh^{-1}\left(\sqrt{\eta}\right)}{\pi d},$$

where η is the maximum reflection efficiency, d is the film thickness, and λ_o is the peak wavelength. Using this formula, Δn was calculated from the efficiency of the holograms (see Figure 3-10). The results show that Δn of up to 0.03 can be achieved. In terms of PWAS parameters, the waveguide channel will have n_{WG}=1.53 while the buffer layer will have n_B=1.5.

No-dye DPP also exhibits very low absorption across the whole visible region (see Figure 2-6), as is necessary for efficient light delivery.

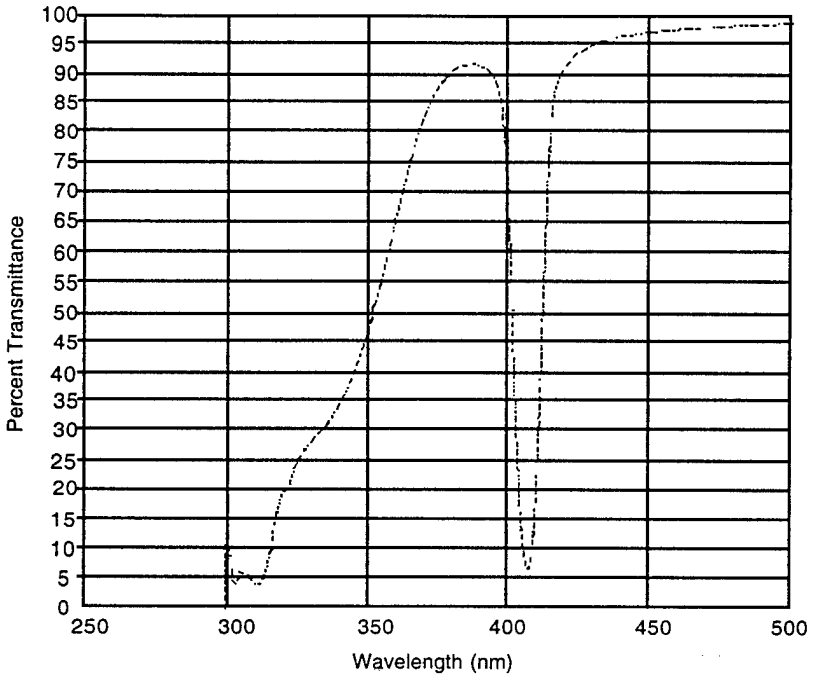

Figure 3-10
No-dye hologram transmission. (Diffraction efficiency η is related to transmittance T by the relation $\eta = 1-T$.)

The film tested was 20 μm thick, and the spectrophotometer beam was ~2 mm in diameter. Under these conditions, the maximum loss at 470 nm in a 6 in. long, 20 μm × 20 μm waveguide was only 5%. POC has demonstrated holographic fabrication of channel waveguide structures (see Figure 2-6). The no-dye DPP material index modulation characteristics are listed in Table 3-2.

Table 3-2. No-Dye Film Holographic Characteristics

Exposure Level (mJ/cm^2)	Peak Wavelength (nm)	Index Modulation
50	409	0.0090
100	409	0.0177
200	413	0.0182
400	413	0.0218
800	413	0.0235
1000	413	0.0301

Using this material, we set up a simple holographic recording system to produce parallel channel patterns with adjustable widths. As shown in Figure 3-11, a Coherent 200 high power krypton ion laser tuned to a wavelength of 415 nm was used to record holographic fringe patterns of widths varying from 20 μm to 200 μm. The setup is a Michelson interferometer, which can produce variable fringe spacing by adjustment of one of the mirrors.

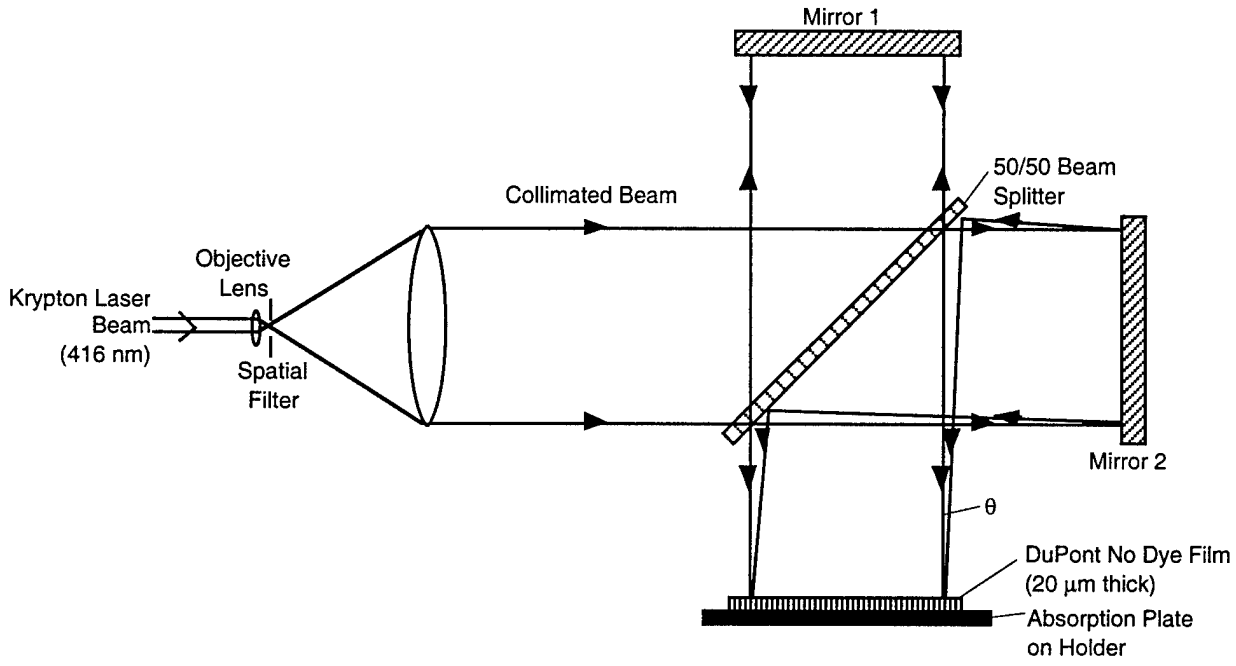

Figure 3-11
Setup for holographic recording of channel waveguides.

An exposure energy of 1000 mJ/cm^2 or higher was used to produce a chopped sinusoidal refractive index profile, a smoothed square wave pattern. The processing of the holographic film involves UV exposure for ~1 minute, followed by baking at ~120°C for about an hour. The fabricated film clearly shows the channel waveguide pattern, and the samples were tested for light propagation using HeNe lasers, laser diodes, and LEDs. The laboratory demonstration of this waveguide is shown above in Figure 2-8.

3.4 Fabrication of LCOS Module

POC investigated various methods of fabricating small array LCOS modules, and tested their performance as an efficient output scanning display device. Both the LC-ROS and the LC-DOS approaches were investigated.

3.4.1 Liquid Crystal Material for LCOS

We surveyed several commercially available nematic liquid crystal (NLC) materials for use in the LCOS demonstration. For this project, the most important consideration is the speed of the NLC molecule orientation response to an electric voltage across the NLC cell.

Four candidate NLCs were purchased from EM Industries, Inc. and studied for this particular application. Their physical properties are listed in Table 3-3.

Table 3-3. Physical Properties of NLC Materials

Property	E7	ZLi1565	MLC-6054-100	MLC-6068-100
$\Delta\varepsilon$	13.8	7.0	26.5	31.6
$\varepsilon_{\parallel}$	19.0	10.7	33.0	39.8
$\varepsilon_{\perp}$	5.2	3.7	6.5	8.21
$\Delta\eta$	0.2253	0.1262	0.1713	0.1531
η_e	1.7464	1.6237	1.6770	1.6541
η_o	1.5211	1.4975	1.5057	1.501
η	59 mm^2s^{-1}	19 mm^2s^{-1}	41 mm^2s^{-1}	60 $mm^{-1}s^{-1}$
K_{11}	11.1 PN	14.4 PN	—	—
K_{22}	—	6.9 PN	—	—
K_{33}	17.1 PN	18.3 PN	—	—
(threshold Vol) V_{10}	1.41 V	2.31 V	1.18 V	1.05 V
(saturation Vol) V_{90}	1.99 V	3.16 V	1.33 V	1.15 V
$\eta/\Delta\varepsilon$	2.82 mm^2s^{-1}	2.71 mm^2s^{-1}	1.55 mm^2s^{-1}	1.90 mm^2s^{-1}

The two NLC type LC materials listed in Table 3-3 have particularly high values of $\Delta\varepsilon$, which give them short response times in accordance with the following equations:

$$Tr = C_1\eta d^2/\left(\varepsilon_o\Delta\varepsilon V^2\right)$$

$$Td = C_2\eta d^2/\left(K_{11}\pi^2\right).$$

Here, *Tr* and *Td* are rise (E-field ON) and decay (E-field OFF) times, respectively. C_1 and C_2 are constants, and *d* is the thickness of the LC cell. The definition of *Tr* indicates that $Tr \propto \eta/\Delta\varepsilon$, which is also listed in Table 3-3. Among these four materials, MLC-6054-100 has the lowest value of $\eta/\Delta\varepsilon$ = 1.55 mm^2s^{-1}, while E7 has the highest: $\eta/\Delta\varepsilon$ = 2.82 mm^2s^{-1}. The rise time of MLC-6068-100 was measured to be ~1 ms in response to a 60 V, 1 kHz square wave across a cell 5 μm thick.

The refractive index of LC depends on the angle between the orientation of the LC molecules and the polarization direction of the light beam. In Figure 3-12, the polarization direction of the light beam in the waveguide layer is perpendicular to the paper plane, and the LC alignment should be parallel to this direction. To orient it in this way, a very thin polyimide layer is coated on top of the ITO side of the waveguide layer, and is rubbed to form an alignment layer for the LC medium. If the rubbing direction is parallel to the polarization direction of the light beam, the refractive index of the LC medium is n_e. Since for LC materials n_e is greater than n_o, n_{LC} must be equal to n_o when the light remains in the waveguide. Therefore, LC material is chosen with $n_e \simeq n_{WG}$ and n_o as low as possible.

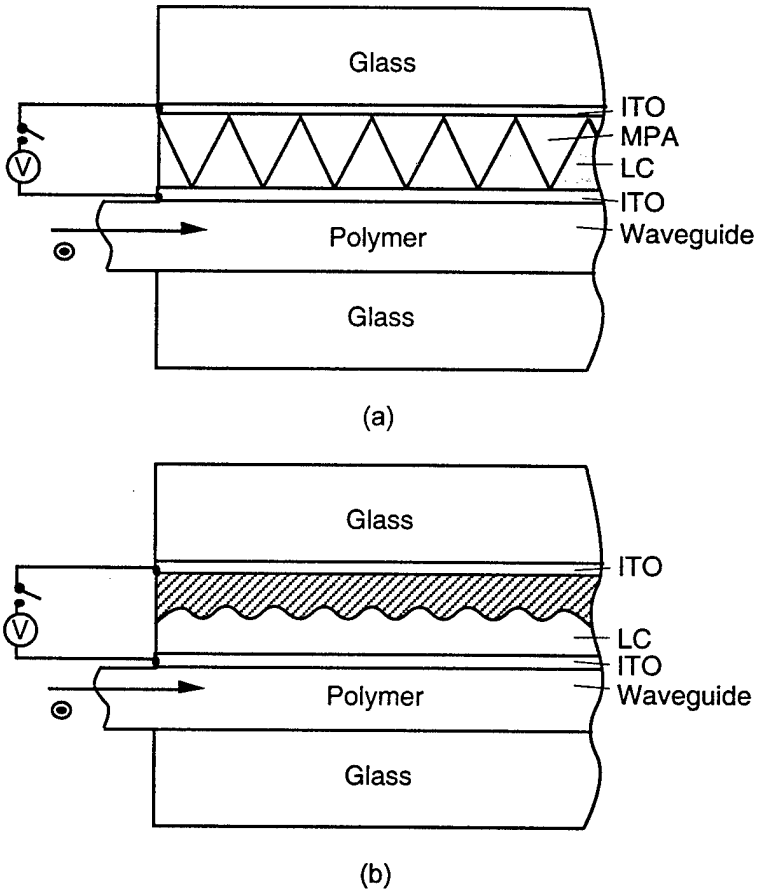

Figure 3-12
Optimized design of LCOS in (a) LC-ROS and (b) LC-DOS configuration.

Next, we consider the response time of the selected LC. Rise time T_r and relaxation time T_d can be expressed as:

$$T_r = C_1 \frac{\gamma d^2}{\varepsilon_o \Delta\varepsilon V^2}, \quad T_d = C_2 \frac{\gamma d^2}{K_{11}\pi},$$

where γ is the rotational viscosity and C_1, C_2 are constants. We see that both T_r and T_d are proportional to γ and to d^2, and that T_r decreases with $\Delta\varepsilon$, while T_d decreases with $K_{||}$. Therefore, we should select LC materials with low viscosity γ, high $\Delta\varepsilon$, and high $K_{||}$, and make the cells as thin as we can.

Nematic LC materials used for display are cross-aligning to form a twisted nematic LC (TNLC) structure. Its switching speed, which is defined as the time required to **rotate** or uncoil the LC molecule, depends very strongly on the viscosity of the LC material and on the applied voltage. On the other hand, LC birefringence (Δn) as a result of **tilting** the molecules is less sensitive to viscosity. This can be seen in the onset of Δn change at very low applied voltage, well below the threshold at which rotation begins. Therefore, LCOS switching occurs within a fraction of the NLC switching time normally specified for LC material. Commercial NLCs are available with ~1 ms speed in the TNLC configuration.

3.4.2 LC Cell Configurations

One of the most important characteristics of an LC device is the cell configuration, which determines the orientation of LC molecules on the cell substrates, i.e., the surface alignment. By correlation among LC molecules, a certain orientation structure (geometry) develops and propagates from the surface substrates into the entire LC cell. Molecules typically align parallel ("homogeneous") or perpendicular ("homeotropic") to the substrate surfaces, as illustrated by Figure 3-13.

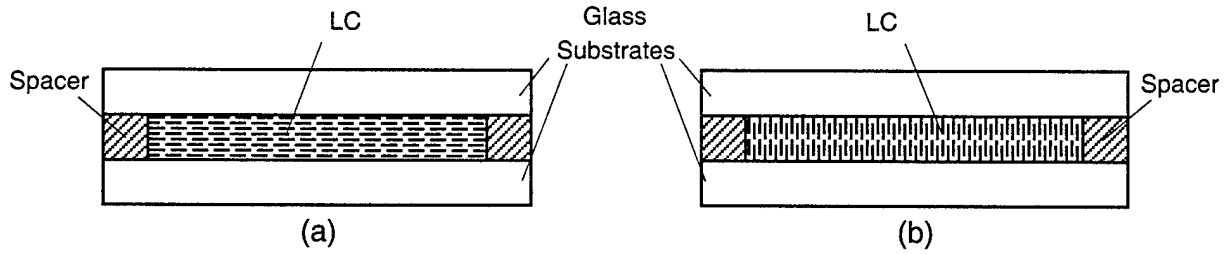

Figure 3-13
Two fundamental types of LC cell configurations with molecular alignments on substrate surface (a) parallel, i.e., homogeneous; (b) perpendicular, i.e., homeotropic.

In the LCOS module, the refractive index of the LC material switches between n_o and n_e when the E-field is switched on and off. The configuration shown in Figure 3-14, with the LC molecules aligned by rubbing the top substrate in the direction indicated by the arrow, is suitable for use in this project.

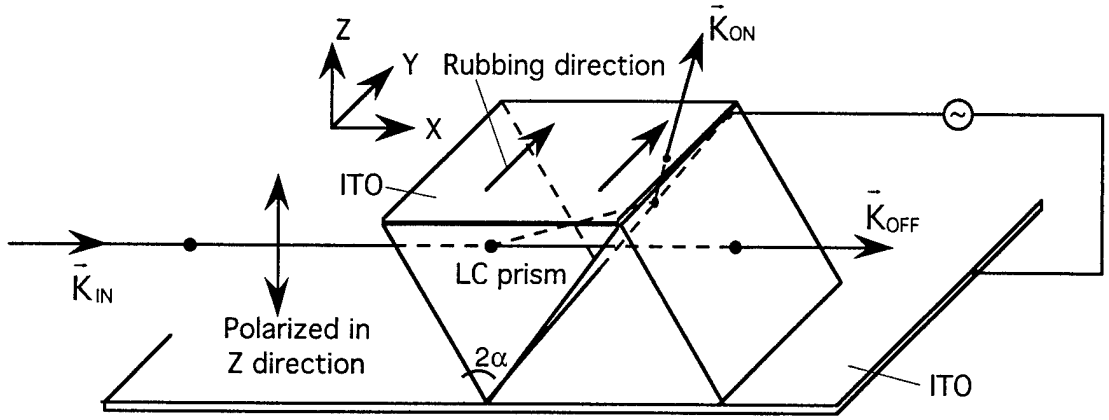

Figure 3-14
Total internal reflection (TIR) occurs when $n_L > n_W$, in the on state; light passes through when $n_L = n_W$, when the electric field is off.

Only one LC microprism and a polymer microprism are shown in Figure 3-14. The electric field across the LC prism (i.e., across one pixel of the LCOS) determines the outgoing direction of the light when the light strikes the interface between the two prisms.

Assume that light linearly polarized in the Z direction propagates in the X direction as shown by $\vec{K}_{IN}$. When the E-field is off, the LC molecules are aligned in the Y direction, perpendicular to the polarization direction of the incident light. The refractive index of the LC microprism is $n_{\perp} \simeq 1.5$, which is equal to that of $n_{polymer}$. This index matching between the two microprisms allows the light to pass through the interface without deflection, as shown by $\vec{K}_{OFF}$. However, when the E-field is on, the molecules are bent to the direction of the E-field ($\Delta\varepsilon > 0$ LC material is used), which is in the Z direction. The refractive index of the LC microprism is $n \simeq n_{||}$. The resulting mismatch of index causes the light beam to be deflected at the interface. We calculated that when the vertex angle of the prism is > 66.22°, total internal reflection (TIR) will occur.

The thickness of the LC cell, approximately the thickness of the microprism array, is about 10 μm. The linear LC array is scanned sequentially in accordance with the raster scanning method typically used in commercially available active matrix LCDs (AMLCDs).

PI2555 polyimide, purchased from DuPont, was studied and used for the surface alignment coating. A spin-coat of the PI2555 solution (4% PI2555 in 96% thinner) was applied to ITO-coated glass. The thickness of the layer depends on the spinning speed. A 1000 - 5000 Å thick PI2555 layer was deposited on top of the ITO layer at a spinning speed between 3000 and 2000 rpm. A one hour oven bake is followed by unidirectional rubbing with a specially designed rubbing cloth, procured from Yoshikawa Chemical Company through Brewer Science, Inc. A uniform homogeneous alignment with a pretilt angle of 2°-4° results from unidirectional rubbing 5 to 10 times.

3.4.3 LCOS Fabrication

The polymer microprism layer can be fabricated on the ITO coated glass substrate by using a special method developed at POC. The microprism array master in quartz is used to produce a flexible submaster prism array, which is then used to produce the microprisms on ITO-coated glass. Figure 3-15 shows the steps in producing an array using Norland NOA 72 optical grade epoxy. NOA 72 has a refractive index of 1.56 when fully cured. It is well known for its high optical quality, and has been used to integrate commercial as well as military optics. The thickness of the polymer microprism can be controlled by the amount of material used for replication. From 1 to 2 drops of NOA 72 covers a 2 in. × 2 in. square, and a microprism ~10 to 20 μm thick can be produced on a piece of ITO-coated glass. Figure 3-16 is a 200× photomicrograph of a 30 μm × 50 μm microprism array.

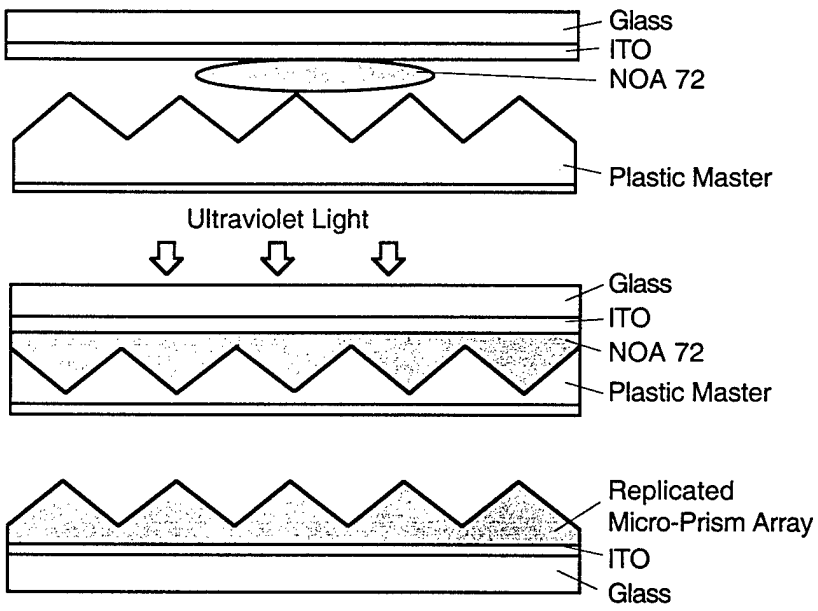

Figure 3-15
Process of replicating microprism array from flexible master, which is generated from an original microprism array, onto ITO-coated glass plate.

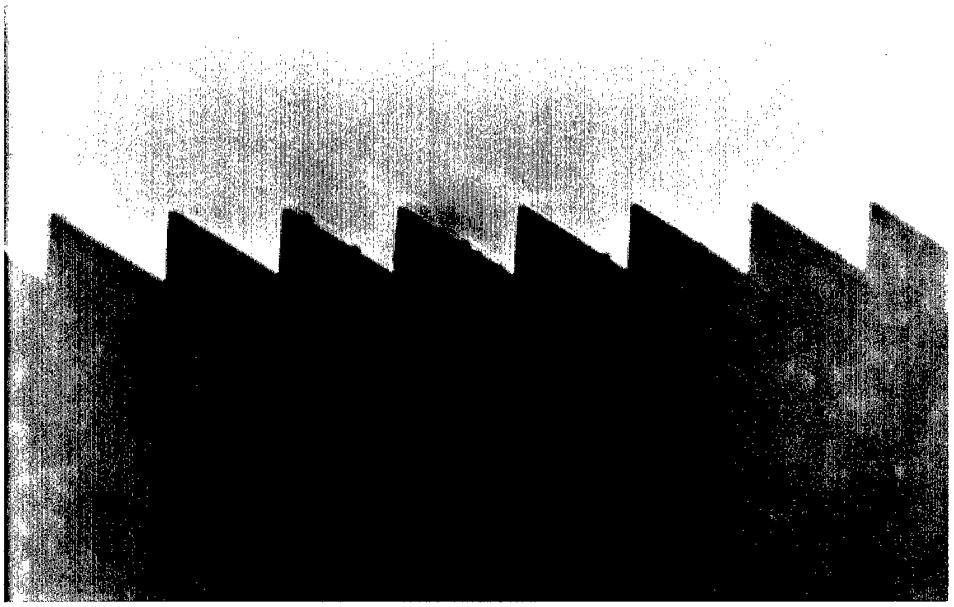

Figure 3-16
Side view of a 30 μm × 50 μm micro-prism array replicated at POC (magnified 200 times).

A unique method was successfully developed for fabricating very thin micro-prism arrays and diffractive/diffuser microstructures inside LCOS cells by optimized epoxy-based replication, based on our proprietary techniques.

3.4.4 High Speed LC for High Resolution GLASS Display

Using an optimized LCOS configuration and commercial NLCs with ~1 ms speed in the TNLC configuration, Δn can be switched within 1/10 to 1/3 of this time; i.e., in 100 μs to 300 μs, which meets the requirement for a high resolution (1280 × 1024) GLASS display. For future development, the most promising NLC or a suitable FLC materials with sufficient Δn should be selected for optimization of LCOS fabrication. Table 4-3 lists a few candidate commercially available LC materials.

Table 4-3. Technical Characteristics of Candidate LC Materials

LC Material		Phase Range (a)	Speed	Drive Voltage
Nematic LC	E7 (b)	-30 to 58°C	10 to 100 ms	~3 V
	MLC6068-100 (b)	-30 to 73°C	10 to 100 ms	~3 V
	ZLi1565 (b)	-42 to 85°C	1 to 10 ms	~3 V
Ferroelectric LC	FELIX-017/100 (c)	-28 to 73°C	~30 μs	Varied, ~10 $V_{pp}/\mu s$
	FLC10150 (d)	-40 to 69°C	~30 μs	Varied, ~6 $V_{pp}/\mu s$

(a) Minimum storage temperature can be a few degrees above the lower end of the phase range.
(b) Product of EM Industries, USA
(c) Product of Hoechst, Germany
(d) Product of Rolic, Switzerland

4.0 CONCLUSIONS AND RECOMMENDATIONS FOR FUTURE WORK

4.1 Conclusion

The Phase I investigations have demonstrated that a practical, commercially viable miniature display can be developed based on POC's novel GLASS display concept. A high resolution version of this unit can be designed, fabricated, and manufactured for Army land warrior night vision HMDs and for high end commercial uses such as medical HMDs, and a lower-priced version for major commercial applications. POC believes that the further development of a full scale GLASS display will lead to the most advanced and lowest cost HMD yet developed.

4.2 Recommendation for Future Work

POC recommends the following further GLASS display development:

- Optimize and refine GLASS display for Army HMD applications, in terms of human factors considerations as well as electronic image data transfer and interface subsystems.
- Develop critical system components, and optimize their fabrication processes as well as system integration technologies.
- Develop a functional low cost, flexible prototype GLASS display unit with performance required by Army HMD systems.
- Test and evaluate performance of prototype GLASS display for HMD application, and deliver the prototype to the government.
- Develop a manufacturing plan for high-volume, low-cost production of GLASS displays.

5.0 APPLICATIONS AND COMMERCIALIZATION

HMD technology advances enabled by successful development of the proposed GLASS display system will lead to cost-effective commercialization. The new HMD system will find numerous real-time 3-D virtual reality applications. Potential markets for compact, low cost HMDs in the private sector include medicine, avionics, education, CAD, portable computing and communication devices, space exploration, and video games. A single generic virtual environment system could be used with a variety of teleoperated systems, such as industrial robotic manipulator arms, mobile surveillance vehicles, and heavy construction equipment. Additional commercial applications include simulation training for hazardous duties such as fire fighting, law enforcement, bomb disposal, and hazardous material handling. By sharing a common virtual environment, many people can be trained to operate collaboratively in virtual air-traffic control systems, virtual command posts, educational and medical training facilities, and entertainment centers. Military applications for HMD displays include pilot and combat vehicle crew training, thermal weapon sights, soldier's integrated protective ensemble and logistics and training applications. This demonstration of a GLASS display system in Phase I has also laid the ground-work for polymer waveguide substrate-based laser scanned displays in HDTV systems.

6.0 REFERENCES

1. H. Girolamo, C. Rash, and T. Gilroy, "Advanced Information Displays for the 21st-Century Warrior," Information Display, 3, 10-17, (1997).
2. R.A. Bett, G.R. Knoles, E.H. Lange, B.J. Pilney, and H.J. Girolamo, "Miniature Flat Panels in Rotary Wing Head Mounted Displays," SPIE Proc. 3058, 125-136, (1997).
3. F.J. Ferrin, "Selecting New Miniature Display Technologies for Head Mounted Applications," SPIE Proc. 3058, 115-124, (1997).
4. D. Lytle (Ed.), "A Radical New Approach to Virtual Reality," Photonics Spectra, p. 48 (August 1994).
5. Technical Data on P7 Virtual Display Module, Reflection Technology, Inc., Waltham, MA.
6. Chen, J. C., and Jüngling, S., "Computation of higher-order waveguide modes by imaginary-distance beam propagation method," Optical and Quantum Electronics, Vol. 26, S100-S205, (1994).
7 Hadley, G. R., and Smith, R. E., "Full-vector waveguide modeling using an iterative finite-difference method with transparent boundary conditions," Journal of Lightwave Technology, Vol. 13, pp. 465-499, (1995).
8. P. Hariharam, Optical Holography, Cambridge University Press, Cambridge, (1984).

POC Physical Optics Corporation

July 23, 1998

Charles Bradford
Night Vision Directorate
ATTN: AMSEM-RD-NV-STD
Fort Belvoir, VA 22060-5806

Reference: Contract DAAB07-98-C-G011
"Miniature Guided Light Array Sequential Scanning Display for Head Mounted Displays"

Dear Mr. Bradford

Enclosed please find two (2) copies of the Final Report, DD882, as well as the corresponding DD250 for the above-referenced contract. Upon your approval of the DD250, please forward a signed copy to me in the envelope provided.

Please feel free to contact me if you have any questions or need additional information.

Sincerely,

Olivia Huang
Legal & Contracts Administrator

OH/pl
Enclosures
cc: Roebuck (DD250)
DTIC (1 each)
Ref: 3443

20600 Gramercy Place, Building 100, Torrance, California 90501 • (310) 320-3088 • FAX (310) 320-4667